

# Soft Matter

Accepted Manuscript



This is an *Accepted Manuscript*, which has been through the Royal Society of Chemistry peer review process and has been accepted for publication.

*Accepted Manuscripts* are published online shortly after acceptance, before technical editing, formatting and proof reading. Using this free service, authors can make their results available to the community, in citable form, before we publish the edited article. We will replace this *Accepted Manuscript* with the edited and formatted *Advance Article* as soon as it is available.

You can find more information about *Accepted Manuscripts* in the [Information for Authors](#).

Please note that technical editing may introduce minor changes to the text and/or graphics, which may alter content. The journal's standard [Terms & Conditions](#) and the [Ethical guidelines](#) still apply. In no event shall the Royal Society of Chemistry be held responsible for any errors or omissions in this *Accepted Manuscript* or any consequences arising from the use of any information it contains.

# Stimuli-responsive Pickering emulsions: Recent advances and potential applications

Juntao Tang, Patrick James Quinlan, Kam Chiu Tam\*

Department of Chemical Engineering, Waterloo Institute for Nanotechnology, University of Waterloo, 200 University Avenue West, Waterloo, ON, N2L 3G1, Canada

## Abstract

Pickering emulsions possess many advantages over traditional surfactant stabilized emulsions. For example, Pickering emulsions impart better stability against coalescence and, in most cases, are biologically compatible and environmentally friendly. These characteristics open the door for their use in a variety of industries spanning petroleum, food, biomedicine, pharmaceuticals, and cosmetics. Depending on the application, rapid, but controlled stabilization and destabilization of an emulsion may be necessary. As a result, Pickering emulsions with stimuli-responsive properties have, in recent years, received a considerable amount of attention. This paper provides a concise, and comprehensive review of Pickering emulsion systems that possess the ability to respond to an array of external triggers, including pH, temperature, CO<sub>2</sub> concentration, light intensity, ionic strength, and magnetic field intensity. Potential applications for which stimuli-responsive Pickering emulsion systems would be of particular value, such as emulsion polymerization, enhanced oil recovery, catalyst recovery, and cosmetics, are discussed.

**Keywords:** Pickering emulsion, stimuli-responsive, nanoparticle, surfactant free, polymer

## 1. Introduction to Pickering emulsions

Emulsions play an important role in a number of industrial processes and commercial products where immiscible liquid phases coexist. Conventionally, emulsions are stabilized by the addition of molecular surfactants or amphiphilic polymers, which adsorb at the oil/water interface and impede the coalescence of emulsified droplets by introducing electrostatic and steric repulsive forces. However, the cost of surfactants is typically high and, in most circumstances, their recovery is not practical<sup>1</sup>. Additionally, it is well known that some surfactants induce tissue irritation and even cell damage, making their use in biomedical applications a major concern<sup>2,3</sup>. In the late nineteenth and early twentieth centuries, Haynes, Bessel, Ramsden and Pickering reported on a new classification

of emulsions, presently termed Pickering emulsions, wherein solid colloidal particles were observed to adsorb at the oil/water interface and provide emulsion stability<sup>3-8</sup>. Because Pickering emulsions retain several of the basic properties of conventional emulsions, they can, in many cases, be substituted for surfactants. This makes them an attractive alternative in a number of industries seeking to avoid the use of surfactants<sup>2,8-10</sup>. They also open the door for new techniques to prepare functional nanomaterials. Throughout the past century, a considerable amount of interest and effort have been devoted to advancing our understanding and development on this interesting system<sup>2,7,8,11</sup>.

The preparation of a Pickering emulsion involves the dispersion of solid particles into the continuous phase of an emulsion, and based on their partial wettability in each of the two immiscible phases, they adsorb at the oil/water interface to form an effective steric and electrostatic protective shield for the emulsified droplets. Pioneering work in the field revealed that the type of emulsion formed, i.e. oil-in-water (o/w) or water-in-oil (w/o) could be predicted based on the preferential wettability of the emulsifier. For particles more easily wetted by the water phase, it was observed that they would reduce their contact with the oil phase, causing the interface to curve and form spherical oil droplets. The opposite would occur for more lipophilic particles. While the size of droplets in traditional surfactant stabilized emulsion systems is typically submicrometer, droplets in Pickering emulsions are frequently on the order of micrometers<sup>12</sup>. Analogous to the hydrophilic-lipophilic balance (HLB) parameter used to describe the preferential wettability of a surfactant molecule at an oil/water interface, the three-phase contact angle of a solid particle situated at an oil/water interface may also be used<sup>1</sup>. The contact angle measured at the water phase,  $\theta_w$ , is given by the Young's equation shown below (Eq. 1):

$$\cos \theta_w = \frac{\gamma_{s/o} - \gamma_{s/w}}{\gamma_{o/w}}$$

where  $\gamma_{s/o}$ ,  $\gamma_{s/w}$ , and  $\gamma_{o/w}$  are the solid/oil, solid/water, and oil/water interfacial energies, respectively. For more hydrophilic particles,  $\theta_w$  is typically less than  $90^\circ$  and the majority of the particle is wetted by the water phase. For more lipophilic particles,  $\theta_w$  is typically greater than  $90^\circ$  and more of the particle surface is wetted by the oil phase. Particles equally wetted by both phases result in  $\theta_w$  being equal to  $90^\circ$ . In such a case, the oil/water interface is effectively planar (Figure 1). Complete wetting of the particle in either phase results in particle instability at the interface. In

this case, the particles become completely dispersed in a single phase, and stable emulsions cannot be achieved<sup>1</sup>. In general, more hydrophilic particles, such as metal oxides and silica, can stabilize o/w emulsions, and more lipophilic particles, such as carbon black, can stabilize w/o emulsions<sup>13-20</sup>. Optimum stability in a Pickering emulsion system may be obtained when the contact angle approaches 90°, but retains some degree of preferential wettability for one phase over the other. In fact, studies by Kaptay<sup>21</sup> suggested that the optimum  $\theta_w$  for stabilizing o/w emulsions is 70-86° and 94-110° for stabilizing w/o emulsions.

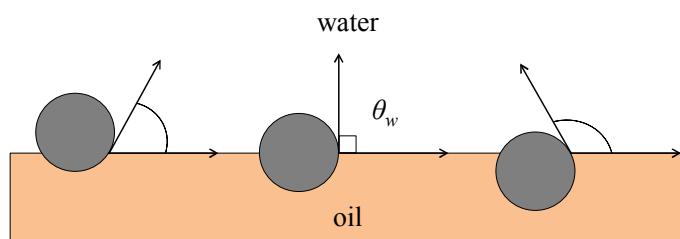


**Figure 1** Position of a small spherical particle at an oil/water interface with a contact angle measured into the water phase of  $< 90^\circ$  (left, hydrophilic), equal to  $90^\circ$  (center, equally hydrophilic and lipophilic),  $> 90^\circ$  (right, lipophilic).

Binks<sup>1</sup> showed that for small particles (less than 2  $\mu\text{m}$ ), gravitational effects may be neglected, such that the amount of energy  $\Delta E$  required to remove a solid spherical particle of radius  $r$  from the oil/water interface is (Eq. 2):

$$\Delta E = \pi r^2 \gamma_{o/w} (1 \pm \cos \theta_w)^2$$

where  $\gamma_{o/w}$  is the oil/water interfacial tension and  $\theta_w$  is the three-phase contact angle measured into the water phase. The sign preceding  $\cos \theta_w$  is negative for particle removal to the water phase and positive for particle removal to the oil phase. From this equation, it may be concluded that the energy of adsorption of a particle at an interface is always greater than the particle's thermal energy, even in the case of very small solid particles. For example, the amount of energy required to remove a 10 nm solid spherical particle from a hydrocarbon/water interface ( $\gamma_{o/w} = 50 \text{ mN}\cdot\text{m}^{-1}$ ,  $\theta_w = 90^\circ$ ) is  $\Delta E = 1.6 \times 10^{-17} \text{ J}$ , which is orders of magnitude greater than  $kT$  ( $4.1 \times 10^{-21} \text{ J}$  at 293 K). Thus, solid particles, once attached to the oil/water interface, can be thought of as irreversibly adsorbed. This is in contrast to surfactant molecules, which adsorb and desorb on a relatively fast timescale<sup>1</sup>. Pickering emulsion stability is influenced by a number of factors, including  $\theta_w$ , particle concentration, particle size and shape, the ratio of oil to water phase, and ionic strength<sup>1</sup>.

There exists a wide variety of Pickering emulsion systems described throughout the literature, spanning inorganic, organic, and hybrid nanoparticles, the details of which are briefly summarized in Table 1. Since the types of Pickering emulsifiers have been reported previously<sup>2,9</sup>, several notable examples are presented here.

**Table 1** A brief summary of Pickering emulsifiers.

Particle type	Particles	Emulsion Type	References	
<b>Inorganic</b>	<b>Silica</b>	Fumed silica	o/w or w/o	1,20
		Carbonyl iron particles	o/w	12
	<b>Metal oxide</b>	Fe <sub>3</sub> O <sub>4</sub> nanoparticles	w/o	13,22
		TiO <sub>2</sub>	o/w	23
		CuO	o/w	24
		<b>Clay</b>	Montmorillonite (MMT)	o/w
	Laponite RD		o/w	26
	Layered double hydroxide (LDH)		o/w	27
	<b>Carbon</b>	Carbon nanotube (CNT)	w/o	28
		Graphene oxide (GO)	o/w	29
Carbon black (CB)		w/o	17,18	
<b>Organic</b>	<b>Protein</b>	Bovine serum albumin coupled with PNIPAM	o/w	30
	<b>Polysaccharide nanocrystals</b>	Cellulose nanocrystals	o/w	14,15,31
		Chitin nanocrystals	o/w	32
		Starch nanocrystals	o/w	33
	<b>Polymeric</b>	Poly(divinylbenzene-methacrylic acid) (P(DVB-MAA)) particles	w/o	34
		Polystyrene (PS) or poly(methyl methacrylate) (PMMA) nanoparticles	w/o	35
		Poly{(styrene- <i>alt</i> -maleic acid)-co-[styrene -(N-3,4-dihydroxyphenylethyl-maleamic acid)]} (P(SMA-Dopa))	o/w	36
	<b>Composite/hybrid</b>	Ag <sub>3</sub> PO <sub>4</sub> /MWNT nanohybrid	w/o	37
Lightly crosslinked Poly(4-vinylpyridine) (P4VP)-Silica Nanocomposite Microgels		o/w	38	

## 2. Stimuli-responsive Pickering emulsion

For some applications, for example bitumen emulsification or food storage, long-term emulsion stability is critical. However, in other cases, such as oil recovery<sup>39</sup>, liquid phase heterogeneous catalysis<sup>40</sup>, and emulsion polymerization<sup>41</sup>, only temporary stability is desired. In these instances, additional physical and/or chemical disruption mechanisms must be introduced into the system to destabilize the emulsion, which demand increased capital and operating costs. In an effort to simplify the demulsification process, much research has been devoted to the development of Pickering emulsifiers that activate and deactivate in response to external stimuli. In many cases, the surface properties of the solid particles undergo some physical or chemical transformation in response to environmental triggers that, in turn, alter the wettability of the particles. This enables the remote control of the emulsion characteristics from the bulk of the system. It also allows for the recovery and reuse of emulsifiers, which helps to achieve a more sustainable operation. In this section, a concise, but comprehensive review of stimuli-responsive Pickering emulsion systems recently reported in the literature is presented.

### 2.1 pH-responsive systems

Special attention has been devoted to the development of pH-responsive Pickering emulsions, as they are one of the simplest and most readily implementable stimuli-responsive systems (Table 2). A particle is considered pH-responsive when its surface chemistry undergoes some type of modification in response to changes in proton concentration<sup>42</sup>, which then alters the way the material interacts with its surroundings. A wide array of materials has been explored as pH-responsive Pickering emulsifiers, including unmodified organic<sup>36,43,44</sup> and inorganic<sup>45,46</sup> nanoparticles, non-covalent<sup>27,47–52</sup> and covalent<sup>53,54</sup> surface functionalized nanoparticles, and self-assembled particles and micelles<sup>6,55–59</sup>.

A number of unmodified nanoparticles possess pH-responsive behavior. For instance, graphene oxide (GO) particles were recently proposed as pH-responsive Pickering emulsifiers by Kim and coworkers<sup>29</sup> (Figure 2). As a result of the carboxylate moieties located on the perimeter of the particles and the overall lipophilicity of their basal plane, GO particles possess amphiphilic properties. The authors reported on the size dependent amphiphilicity of GO, concluding that small sheets ( $\leq 1 \mu\text{m}$ ) were hydrophilic enough to stabilize o/w emulsions for extended periods of

**Table 2** pH-responsive Pickering emulsion systems

Particles	Modifiers	References
Layered double hydroxide (LDH)		27
Graphene Oxide		29
P(SMA-Dopa) random copolymer		36
P4VP-SiO <sub>2</sub> composites		38
Colloidal particles from the water-insoluble protein zein		43
Chitosan NPs		44
Montmorillonite	$\gamma$ -methacryloxy propyl trimethoxysilane	46
Hydroxyapatite NPs		45
Alumina-coated silica NPs (Ludox CL)	Potassium hydrogen phthalate (KHP)	47
PS latex	PMMA-PDMA as stabilizer	48
PS latex	PMMA-PDMA as stabilizer *	49
Silica NPs	8-hydroxyquinoline (8-HQ)	50,52
Alumina or silica colloids	Poly(methacrylic acid sodium salt) & poly(allylamine hydrochloride)	51
Silica NPs	Mixed organosilanes	53
Silica NPs	P(St- <i>b</i> -2VP- <i>b</i> -EO)	54
P(tert-butylaminoethyl methacrylate) latex		55
P(2-(tert-butylamino) ethyl methacrylate) (PTBAEMA) microgel		56
Self-assembled micelle	P(EO- <i>b</i> -GMA- <i>b</i> -DEA)	57
Self-assembled particles	PU- <i>g</i> -PDEM	58
PS-PAA Janus particles		59
Colloidal silica particles	Sulfonated poly(styrenesulfonate)	60
Opposite charged microgel P(NIPAM-MAA) and P(NIPAM-AEM)		61
Alkaline lignin		62
Partially hydrophobic silica NPs		63
Mg(OH) <sub>2</sub> NPs		64
P(St- <i>alt</i> -MAN)- <i>co</i> -P(VM- <i>alt</i> -MAN) *	Self-assembled and crosslinked particle	65
Fe <sub>3</sub> O <sub>4</sub> NPs	Coated with oleic acid	66
Alginate	Chitosan	67
Silica NPs	Mixed brush	68

\* **PMMA-PDMA**: Poly(Methyl methacrylate)-poly(2-(dimethylamino)ethyl methacrylate); **P(St-*alt*-MAN)-*co*-P(VM-*alt*-MAN)**: Poly-(styrene-*alt*-maleic anhydride)-*co*-poly (7-(4-vinylbenzyloxy)-4-methylcoumarin-*alt*-maleic anhydride); **NPs**- nanoparticles

time, i.e. months, in neutral pH. Acidification of the aqueous phase reportedly resulted in protonation of the edge-bound carboxylates on GO. This caused the particles to be ejected from the interface into the oil phase, resulting in emulsion destabilization and macrophase separation. Similarly, the addition of strong base caused the GO to become more hydrophilic and for  $\text{pH} > 10$ , the particles were observed to migrate to the aqueous phase, again resulting in droplet coalescence. Liu and coworkers<sup>44</sup> investigated the use of chitosan nanoparticles to stabilize a variety of o/w emulsions, e.g. liquid paraffin, *n*-hexane, toluene, and dichloromethane. The authors observed that for neutral and basic conditions, i.e.  $\text{pH} > 6$ , the particles were able to provide emulsion stability for greater than two months. Acidification, however, resulted in particle removal to the aqueous phase resulting in rapid demulsification. The pH-responsive behavior of the particles was attributed to the protonation and deprotonation of the primary amine groups on deacetylated chitosan monomers under acidic and mildly basic conditions, respectively.

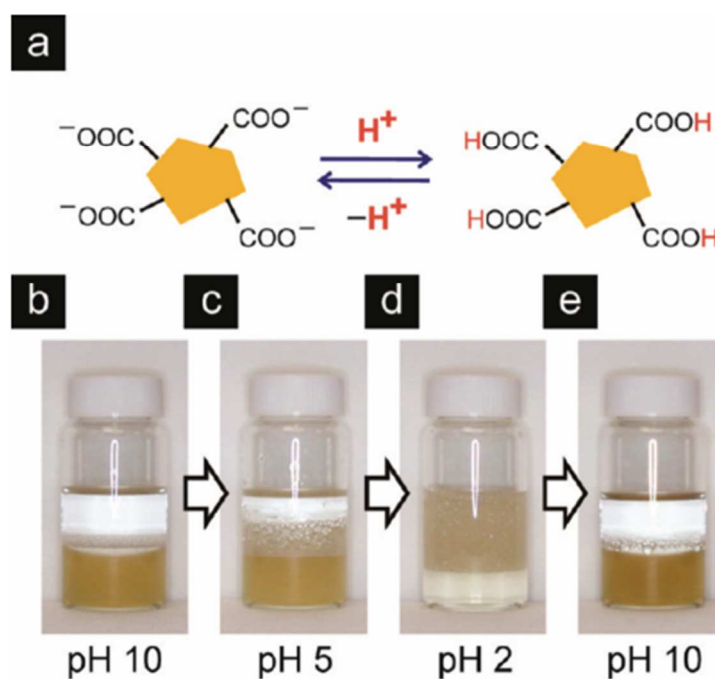


**Figure 2** (a) Schematic illustration demonstrating the pH-responsive amphiphilicity of GO resulting from protonation and deprotonation of edge-bound carboxylate moieties; (b-e) Digital photographs demonstrating the pH-responsiveness of a toluene-in-water emulsion stabilized by GO Reprinted with permission from American Chemical Society (ref. 29), Copyright (2010).

While some nanoparticles alone, such as those discussed above, possess pH-responsive surface

behavior, surface functionalization is one way of rendering non-responsive particles with a broad range of pH-responsive properties. The modification of nanoparticles may be achieved through non-covalent, i.e. electrostatic interactions, hydrogen bonding, and van der Waals forces, or covalent bonding. Li and Stöver<sup>47</sup> (Figure 3) described a simple and reversible emulsifier based on the interaction between commercially available alumina-coated silica nanoparticles (Ludox CL) and the small molecule potassium hydrogen phthalate (KHP). Under mildly acidic conditions, i.e.  $3.5 \leq \text{pH} \leq 5.5$ , the negatively charged KHP bound reversibly with the positively charged nanoparticle surface, rendering the particles partially hydrophobic. Under strongly acidic conditions, the KHP was primarily present in its protonated form and the electrostatic driving force for binding was eliminated. Similarly, under neutral and basic conditions, the deprotonation of the nanoparticles diminished the nanoparticle-KHP binding. In the absence of KHP binding, the nanoparticle surface was observed to be strongly hydrophilic and was no longer stable at the oil/water interface. Amalvy et al.<sup>48,49</sup> successfully synthesized well-defined tertiary amine methacrylate-based block copolymers that adsorbed onto polystyrene latex nanoparticles, with the hydrophobic block bound on the particle surface and hydrophilic segment directed outward to provide steric stabilization. The prepared functionalized latexes were employed as Pickering emulsifiers for stabilizing o/w emulsions. They attributed the pH-responsive functionality to the presence of the steric stabilizer, which, under neutral conditions, possessed an affinity for the oil phase. Acidification of the system resulted in the desorption of the particles from the interface, resulting in droplet coalescence. Haase et al.<sup>52</sup> (Figure 4) also reported on a pH-responsive Pickering emulsion system that could stabilize o/w emulsions within a narrow pH window ( $4.5 \leq \text{pH} \leq 5.5$ ). The stabilization of oil droplets was achieved by increasing the hydrophobicity of silica particles (Lumox TMA) through electrostatically driven adsorption of 8-hydroxyquinoline (8-HQ) onto the particle surface. However, when the pH was increased beyond 5.5, insufficient adsorption of 8-HQ resulted in unstable emulsions. Lowering the pH to 4.4 caused the formation of an 8-HQ bilayer on the particle surface, resulting in rehydrophilization and emulsion destabilization. The authors also reported a size dependency of the emulsion droplets as a function of pH. For  $\text{pH} > 5.5$ , a monomodal size distribution was observed, with the droplets on the order of 12  $\mu\text{m}$  in diameter. Reduction in pH resulted in the presence of smaller droplets on the order of 4  $\mu\text{m}$  in diameter. This bimodal distribution existed for  $4.5 \leq \text{pH} \leq 5.5$ . For  $\text{pH} < 4.5$ , a monomodal size distribution was observed, with only the smaller droplets present. These changes in droplet size reflect the observed changes in the emulsifier particle surface as a function of pH. In another work, Haase et al.<sup>51</sup> modified alumina

and silica particles with the weak polyelectrolytes poly(methacrylic acid sodium salt) and poly(allylamine hydrochloride). The affinity of modified particles to the oil/water interface was influenced by the dissociation and thickness of the adsorbed polyelectrolyte layer. The authors claimed that the dependence of the droplet size on pH and the thickness of coating layer could be explained by particle aggregation, particle wetting, and oil phase polarity.

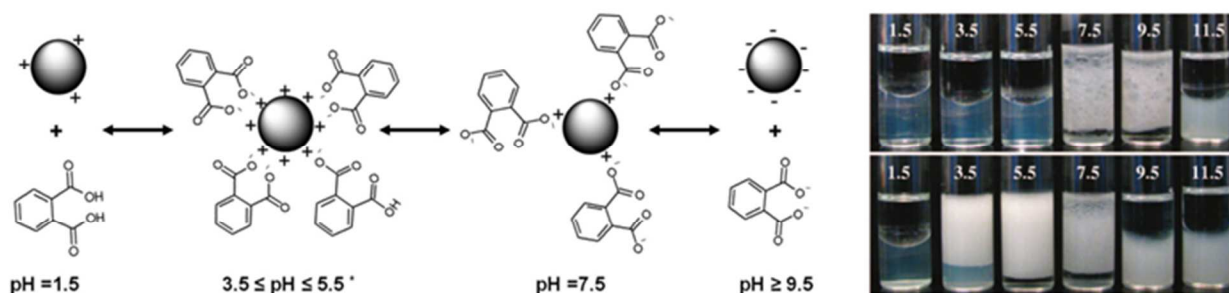


**Figure 3** (Left) Schematic illustration demonstrating the pH-responsive interaction between Ludox CL nanoparticles and KHP. (Right) Digital photographs demonstrating the pH-responsiveness of xylene-in-water emulsions stabilized by Ludox CL nanoparticles in the absence (upper row) and presence (lower row) of KHP Reprinted with permission from American Chemical Society (ref. 47) Copyright (2008).

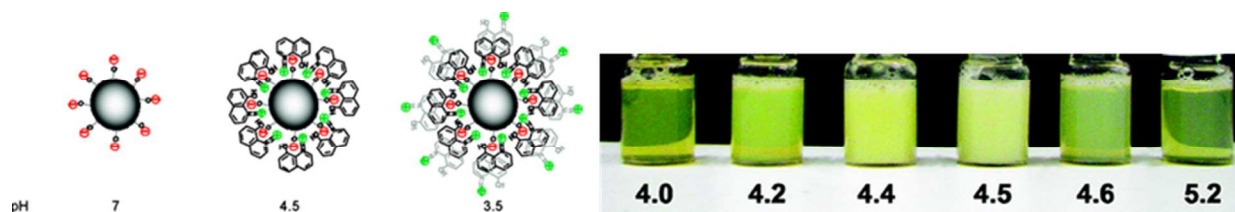


**Figure 4** (Left) Schematic illustration demonstrating the pH-responsive interaction between Ludox TMA nanoparticles and 8-HQ. (Right) Digital photographs demonstrating the pH-responsive stability of Ludox TMA solutions in the presence of 8-HQ Reprinted with permission from American Chemical Society (ref. 52) Copyright (2010).

Yang et al.<sup>53</sup> investigated the covalent surface functionalization of silica microspheres with organosilanes for use as heterogeneous solid catalysts that could repeatedly be separated and recycled by phase transfer (Figure 5). Both the hydrophobic  $(\text{MeO})_3\text{Si}(\text{CH}_2)_7\text{CH}_3$  and the relatively hydrophilic and pH-responsive  $(\text{MeO})_3\text{SiCH}_2\text{CH}_2\text{CH}_2(\text{NHCH}_2\text{CH}_2)_2\text{NH}_2$  were surface grafted onto the particles. By varying the molar ratio of hydrophilic and hydrophobic organosilane brushes, the

authors obtained the desired surface chemistry for in-situ separation and recycling of submicrometer-sized solid catalysts simply by tuning the emulsion pH. The emulsion catalysis system displayed good reversibility in response to pH and a high yield for hydrogenation of styrene after 36 reaction cycles. Motornov et al.<sup>54</sup> also reported a brush-grafted nanoparticle system (Figure

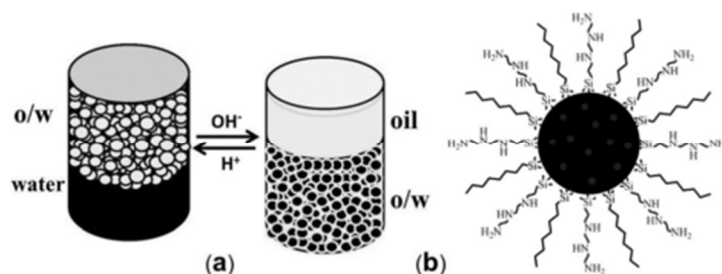


**Figure 5** (a) Schematic illustration demonstrating the pH-responsive phase inversion of emulsions stabilized by organosilane-functionalized silica microspheres; (b) Combinatory organosilane grafting strategy using  $(\text{MeO})_3\text{Si}(\text{CH}_2)_7\text{CH}_3$  and  $(\text{MeO})_3\text{SiCH}_2\text{CH}_2\text{CH}_2(\text{NHCH}_2\text{CH}_2)_2\text{NH}_2$  Reprinted with permission from John Wiley and Sons (ref. 53) Copyright (2013).

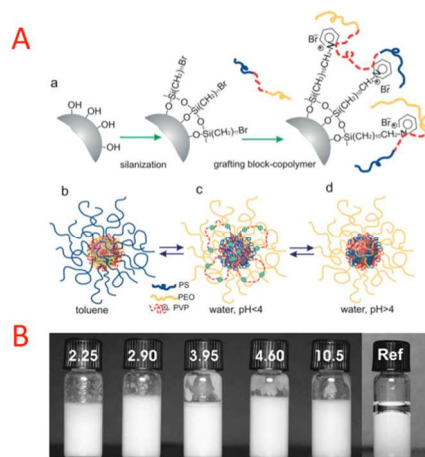


**Figure 6** (A) (a) Strategy used to graft copolymers onto the surface of silica nanoparticles; (b-d) schematic illustration demonstrating the solvent and pH-responsiveness of the copolymer-functionalized nanoparticles. (B) Digital photographs of toluene-in-water emulsions stabilized by P(S-*b*-2VP-*b*-EO) surface grafted silica nanoparticles over a range of pH values Reprinted with permission from John Wiley and Sons (ref. 54), Copyright (2007).

6). Silica nanoparticles were surface grafted with the multifunctional triblock copolymer, poly(styrene-*block*-2-vinyl-pyridine-*block*-ethylene oxide) (P(S-*b*-2VP-*b*-EO)). The emulsions

could undergo o/w to w/o transitions in response to pH changes, allowing for direct control over the emulsion stability. Under acidic conditions, i.e.  $\text{pH} < 3$ , o/w emulsion could be stabilized as a result of the protonation of the P2VP block, making the particle surface more hydrophilic. Adjusting the pH to more neutral and basic conditions, i.e.  $\text{pH} > 4$ , caused deprotonation of the P2VP block, which resulted in a more lipophilic particle surface, causing the observed o/w to w/o phase inversion.

Pickering emulsifiers derived from self-assembled structures or crosslinked microgels have also shown the ability to stabilize and destabilize emulsions in response to pH changes<sup>6,55-59</sup>. Fujii et al.<sup>57</sup> successfully synthesized a poly[(ethylene oxide)-*block*-glycerol monomethacrylate-*block*-2-(diethylamino)ethyl methacrylate] (P(EO-*b*-GMA-*b*-DEA)) triblock copolymer using ATRP, which was observed to self-assemble into micelles in aqueous solution (Figure 7). Crosslinking the shell (PGMA block) of the micelle via amidation reaction with succinic anhydride (SA) yielded core-shell nanoparticles, with the hydrophobic PDEA blocks located within the core of the micelle. PSAGMA and PEO blocks composed the inner and outer coronas of the particle, respectively. These shell crosslinked (SCL) micelles were used to stabilize o/w emulsions at pH 8-9. Acidification of the system caused the emulsion to rapidly coalesce. The authors attributed the demulsification behavior to the protonation of the PDEA core, which caused the particles to swell into cationic nanogels, resulting in the detachment of SCL from the oil/water interface. Ma et al.<sup>58</sup> reported on the design and use of an amphiphilic polyurethane-*graft*-poly[2-(dimethylamino)ethyl methacrylate] (PU-*g*-PDEM) copolymer that self-assembled in water to form core-shell nanoparticles, with the hydrophobic PU blocks bound within the core and the hydrophilic PDEM blocks radially directed outward (Figure 8). The PDEM side chains on the shell were observed to undergo conformational changes into a collapsed state in response to increasing pH. This inhibited the adsorption of nanoparticles onto the interface due to changes in the wettability, inducing demulsification. Thus, w/o emulsions with average droplet size of 10  $\mu\text{m}$  can be found for pH 8-9, while o/w emulsions with average droplet size of 30-40  $\mu\text{m}$  may be observed for  $\text{pH} > 9$  or  $\text{pH} < 5$ . At pH 7, coalescence became apparent after 24 hours. Tu and Lee<sup>59</sup> fabricated amphiphilic polymeric Janus particles, with one side predominantly comprised of hydrophobic styrene and the other consisting of the hydrophilic, pH-responsive acrylic acid. The authors demonstrated that the Janus particles could alter their aggregation and dispersion behaviors in response to changes in pH. Under acidic conditions, the acidic surface of the particles is protonated, allowing the particles to be



conditions, the acrylic acid undergoes deprotonation, which stabilizes o/w emulsions. It was observed that the droplet size for the o/w emulsion was much greater than those observed in the w/o emulsions. The authors attributed this phenomenon to the strong electrostatic charge repulsion between Janus particles in alkaline conditions.

In general, pH-responsive Pickering emulsion systems benefitted from their simplicity and breadth of chemicals and materials available for use. In all cases, simply tuning the pH of the system results in some change in the surface behavior of the particles caused by the protonation or deprotonation of pH-responsive functional groups. Non-functionalized pH-responsive nanoparticles, such as GO<sup>29</sup> and chitosan<sup>44</sup>, may be prepared with relative ease and minimal cost. This opens the door for their use in a range of industrial applications, where large quantities of emulsifier would be required. Further, because these emulsifier systems do not rely on complexation with small molecules or polymers to elicit pH-responsiveness, their stability and usable lifetime are enhanced, lending to more sustainable emulsifier recyclability. Composite emulsifiers, such as surface-functionalized nanoparticles<sup>53,54</sup> and self-assembly systems<sup>6,55-59</sup>, often require more intensive procedures for preparation. Ultimately, it is expected that this would result in a higher material cost, perhaps limiting their applications. However, they also have the potential to be tailored for specific situations, wherein precise control or a narrow transition range is desired. For certain high-value applications, the ability to prepare tailored emulsifier particles may warrant their use.

While pH-responsive systems are simple, well-studied, and diverse, most encounter a number of limitations with respect to their applicability. For instance, the cyclability of these systems may be limited to some finite value due to the inherent increase in the ionic strength of the solution caused by repeated addition of acid and base. The increased addition of free ions in colloidal systems above a critical concentration often results in a phenomenon known as “salting out”, wherein the electrostatic repulsion that stabilizes dispersed colloidal particles in solution is shielded and no longer remains effective<sup>47</sup>. This triggers aggregation of the particles, causing them to lose their functionality as emulsifiers. Another limitation of pH-responsive systems is their inability to be applied in sensitive environments, such as biological systems<sup>43,44</sup>. Furthermore, the addition of acid or base to control the properties of emulsions alters the total volume of the system, diluting the chemical species already present. In many cases, this may be undesirable for the operator. While this would likely remain insignificant for high-volume systems, it may be appreciable for systems of lower volume.

## 2.2 Thermo-responsive systems

Temperature is another commonly investigated stimulus used to control Pickering emulsion stability. While pH adjustment requires the direct addition of acid or base to an emulsion, temperature adjustments may be easily applied without directly affecting the chemical composition of the system. This is an attractive approach for systems sensitive to pH or ionic strength. Some of the strategies used to design pH-responsive systems can similarly be applied to thermo-responsive systems. Thermo-responsiveness is commonly achieved by surface grafting with polymers that exhibit well-documented thermo-responsive properties, such as poly[2-(dimethylamino)ethyl methacrylate] (PDMAEMA), poly(N-isopropylacrylamide) (PNIPAM), and poly(oligo-ethylenoxide) methacrylates (Table 3).

**Table 3** Thermo-responsive Pickering emulsions

Particles	Modifiers	References
PS latex	PMMA-PDMA	69
PNIPAM microgel	PDMAEMA	70
Silica nanoparticles	PDMAEMA	71
PS latex	PNIPAM	72
PNIPAM and P(NIPAM-MAA) microgels		73
PNIPAM microgel		74
Cellulose nanocrystal (CNC)	PNIPAM	75

Binks et al.<sup>69</sup> were among the first to describe a system that used temperature as a trigger to modulate Pickering emulsion stability. They reported on polystyrene (PS) latex particles sterically stabilized by a monodisperse diblock copolymer, poly[2-(dimethylamino)ethyl methacrylate-*block*-methyl methacrylate] (PDMAEMA-*b*-PMMA). The hydrophobic PMMA block was anchored onto the surface of the latex particles by physical adsorption and the free PDMAEMA block was used to tune the surface properties of the particle. PDMAEMA homopolymer exhibits a lower critical solution temperature (LCST) between 32 to 46°C, above which the polymer becomes immiscible in aqueous solution<sup>81</sup>. By increasing the temperature, the polymer-coated particles were observed to increase in hydrophobicity, causing emulsion inversion from o/w to w/o. The average size of the particles was observed to increase from 76 to 113  $\mu\text{m}$  as the temperature of the system increased from 25 to 50°C, the temperature in which emulsion inversion was observed. For temperatures

greater than 50 °C, the w/o droplets were observed to be smaller than the o/w droplets observed below the LSCT. Saigal et al.<sup>71</sup> reported on similar studies, wherein o/w emulsions were stabilized by PDMAEMA surface grafted SiO<sub>2</sub> nanoparticles. ATRP was used to polymerize PDMAEMA brushes from the nanoparticle surface. The authors observed a critical flocculation temperature (CFT) of approximately 50°C, which resulted in the rapid destabilization of emulsions at elevated temperatures. A variety of environmental factors, such as grafting density, pH, ionic strength, and oil phase composition, were observed to influence the stability of the emulsions. Due to its biocompatibility and sharp temperature-induced phase transition, PNIPAM is another thermo-responsive polymer that has been explored as a surface modifier of nanoparticles for Pickering emulsion systems. The amide groups present on PNIPAM make it water-soluble when the solution temperature is below 32°C, but insoluble above this temperature. The driving force for precipitation at high temperature is the entropy gained by the release of water molecules that are partially immobilized by the isopropyl moieties of PNIPAM. Tsuji et al.<sup>72</sup> investigated the surface initiated graft polymerization of PNIPAM from polystyrene (PS) nanoparticles to produce thermo-responsive Pickering emulsifiers. The particles reportedly were able to stabilize a variety of o/w emulsions for more than three months at room temperature. However, microscopic phase separation was observed to occur immediately when the temperature was increased to 40°C, at which point the surface grafted PNIPAM would undergo a coil-to-globule transition, leading to particle instability at the interface. In a study by Zoppe et al.<sup>75</sup>, PNIPAM was grafted to the surface of cellulose nanocrystals (CNC) via surface-initiated single-electron transfer living radical polymerization (SI-SET-LRP). The resulting particles were found to be extremely stable at the oil/water interface, maintaining emulsion stability for up to four months at room temperature. Again, the emulsions were observed to rapidly destabilize at temperatures above the LCST of PNIPAM.

Thermo-responsive systems generally benefit from the fact that temperature is an intensive variable. The temperature of the system may be easily altered without changing its volume or composition. This is particularly useful when a high degree of cycling is required. Emulsions may be stabilized, destabilized, and inverted, all without changing the pH and chemical makeup of the system. Biphasic emulsion-stabilized catalysis, wherein the contents of the system undergo repeated cycling, is one application where non-invasive stimuli, such as temperature, would be of particular interest. An apparent limitation to thermo-responsive systems, however, is the energy requirements for controlling the temperature of the system. For systems of greater volume, the amount of energy

required for heating and cooling becomes much more appreciable. However, many thermo-responsive Pickering emulsifier systems may be tailored to have relatively low temperature transitions close to ambient conditions, potentially reducing the energy requirements of the system.

**Table 4** CO<sub>2</sub>-responsive Pickering emulsions

Particles	Modifiers	References
Silica nanoparticles	N'-dodecyl-N,N-dimethylacetamide	76
Silica nanoparticles	N,N-dimethylacetamide dimethylacetal	77
Lignin nanoparticles	PDEAEMA	78
PDEAEMA latex	PEGMA	79
Crosslinked polymer particles	PDEAEMA	80

### 2.3 CO<sub>2</sub>-responsive Pickering emulsion systems

CO<sub>2</sub> is a unique stimulus for emulsion control in that it is typically low cost, widely available, benign, biocompatible, and simple to implement. When sparged into solution, CO<sub>2</sub> exists as a dissolved gas in equilibrium with carbonic acid. The increase in acidity, similar to the pH-responsive systems previously described, allows for certain chemical moieties on the surface of particles to undergo some type of ionic or conformational change, altering the wettability of the particles. The CO<sub>2</sub> can just as easily be removed by sparging another gas into the system, such as air or N<sub>2</sub>, which helps to strip the dissolved CO<sub>2</sub> from the solution<sup>41,82</sup>. In contrast to pH adjustment, the addition and removal of CO<sub>2</sub> is a non-accumulative process. Therefore, acidification-neutralization cycling may be completed without observing any significant increase in the ionic strength of the system. Table 4 outlines a number of CO<sub>2</sub>-responsive Pickering emulsion systems reported recently in the literature.

Jiang and coworkers<sup>76</sup> investigated the stabilization of o/w emulsions using silica nanoparticles surface decorated with *N'*-dodecyl-*N,N*-dimethylacetamidinium bicarbonate, a CO<sub>2</sub>-responsive surfactant. At low CO<sub>2</sub> concentrations, the surfactant was present in its neutral form, *N'*-dodecyl-*N,N*-dimethylacetamide and the negatively charged silica nanoparticles unable to stabilize o/w emulsions due to their excessive hydrophilicity (Figure 9). Upon the addition of CO<sub>2</sub> to the system at 0-5°C, the surfactants were observed to transform from their neutral amidine form to their positively charged amidinium form. This resulted in the electrostatic adsorption of the surfactants

on the surface of silica nanoparticles, quenching their negative surface charge and allowing for the particle-surfactant complexes to adsorb at the oil/water interface and stabilize the emulsion. Sparging  $N_2$  or air into the system at  $65^\circ\text{C}$  caused the surfactants to revert back into their neutral amidine form, eliminating the electrostatic attraction binding them to silica. This resulted in the desorption of the surfactant from the particles, destabilization of the particles at the interface, and, ultimately, demulsification and macrophase separation. Liang et al.<sup>77</sup> reported on two  $\text{CO}_2$ -responsive system systems, one of which was composed of *N,N*-dimethylacetamine dimethyl acetal (DMADMA) grafted silica particles and the other DMADMA and phenyl co-grafted silica particles. The first, due to the high DMADMA content, possessed a more hydrophilic surface and were able to stabilize o/w emulsions under neutral conditions. Addition of  $\text{CO}_2$  resulted in rapid demulsification, as the particles were ejected to the aqueous phase. The observed particle instability

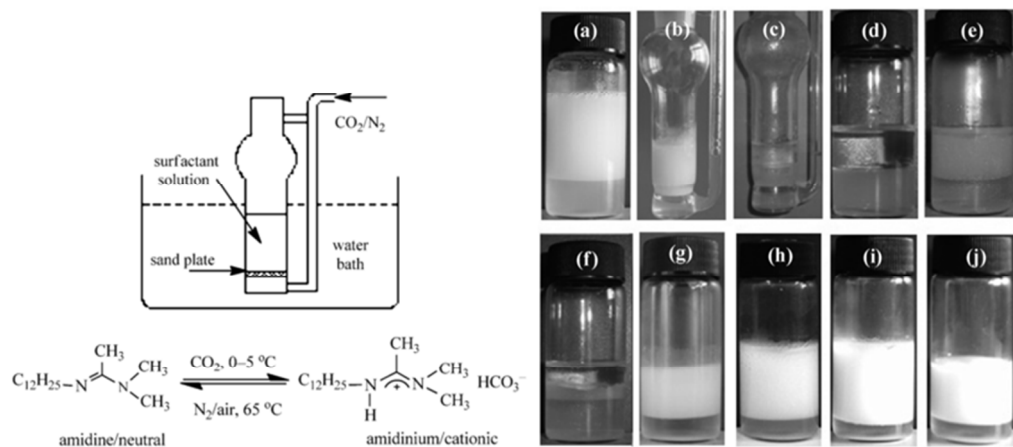


**Figure 9.** (Top-left) Schematic illustration of a temperature controlled gas bubbling device. (Bottom-left) Schematic demonstrating the  $\text{CO}_2/\text{N}_2$ -responsive conversion between *N*'-dodecyl-*N,N*-dimethylacetamide and *N*'-dodecyl-*N,N*-dimethylacetimidium. (Right) Digital photographs demonstrating the  $\text{CO}_2/\text{N}_2$ -responsiveness of *n*-octane-in-water emulsions stabilized by silica nanoparticles and either *N*'-dodecyl-*N,N*-dimethylacetimidium (a-h) or cetyltrimethylammonium bromide (CTAB) (i, j); (a) Amindinium stabilized emulsion; (b-d) Before, during, and after  $\text{N}_2$  bubbling; (e, f) Directly and one week after homogenization; (g, h) Directly and 24 h after  $\text{CO}_2$  bubbling; (i, j) CTAB stabilized emulsion before and after  $\text{N}_2$  bubbling Reprinted with permission from John Wiley and Sons (ref. 76), Copyright (2013).

was attributed to DMADMA protonation. The second and more hydrophobic particles were able to

stabilize w/o emulsions. Destabilization was also observed for this system upon CO<sub>2</sub> addition. In both cases, sparging with air or N<sub>2</sub> reversed the effects observed under CO<sub>2</sub> addition and stable o/w and w/o emulsions could again be achieved. Zeta potential was used to confirm the role of particle surface charge in dictating their surface activity. Qian and coworkers<sup>78</sup> used ATRP to graft PDEAEMA onto the surface of water insoluble lignin nanoparticles. Stable o/w Pickering emulsions were obtained by homogenizing decane in water, in the presence of the PDEAEMA grafted lignin nanoparticles. Within 10 minutes of CO<sub>2</sub> sparging, the droplets were observed to coalesce. In similar fashion to the previously described system, acidification by CO<sub>2</sub> addition resulted in DEAEMA protonation, making the particles more hydrophilic and, thus, unstable at the interface.

Sterically stabilized poly(ethylene glycol) methacrylate-*co*-poly(2-(diethylamino)ethyl methacrylate) (PEGMA-PDEAEMA) latex particles were synthesized by Morse and coworkers via emulsion copolymerization (Figure 10)<sup>79</sup>. The latex particles were observed to behave as pH-responsive Pickering emulsifiers. Similar to previous CO<sub>2</sub>-responsive systems, the authors observed that the emulsion could be demulsified by sparging with CO<sub>2</sub>. The acidification that resulted from CO<sub>2</sub> addition induced the protonation of DEAEMA blocks, causing the latex particles to transform into swollen microgels. These swollen particles were observed to desorb from the oil/water interface, causing the emulsion droplets to coalesce and eventual phase separate. However, subsequent sparging of N<sub>2</sub> caused the microgels to revert back into their denser, more hydrophobic morphology. Interestingly, the authors were unable to observe the restoration of the Pickering emulsion after homogenizing the mixture. They attributed the non-reversibility of the system to the insufficient pH increase by N<sub>2</sub> sparging alone. Liu and coworkers<sup>80</sup> synthesized crosslinked polymer particles via surfactant-free emulsion copolymerization of 2-(diethylamino)ethyl methacrylate (DEAEMA) and sodium methacrylate (SMA) using *N,N'*-methylenebis(acrylamide) (MBA) as a crosslinker. The zwitterionic particles with a unique isoelectric point in the pH range of 7.5-8.0 were introduced into a mixture of dodecane and water (Figure 11). Stable emulsions were prepared under neutral conditions. The emulsions displayed switchable behavior in response to CO<sub>2</sub>/N<sub>2</sub> sparging. Rapid demulsification was observed during CO<sub>2</sub> addition and efficient re-emulsification was observed upon CO<sub>2</sub> removal with N<sub>2</sub> purging. The simple reversibility and stability during cycling, along with the ability to avoid ion accumulation, demonstrate the attractiveness of CO<sub>2</sub>-responsive Pickering emulsion systems across a wide range of industries.

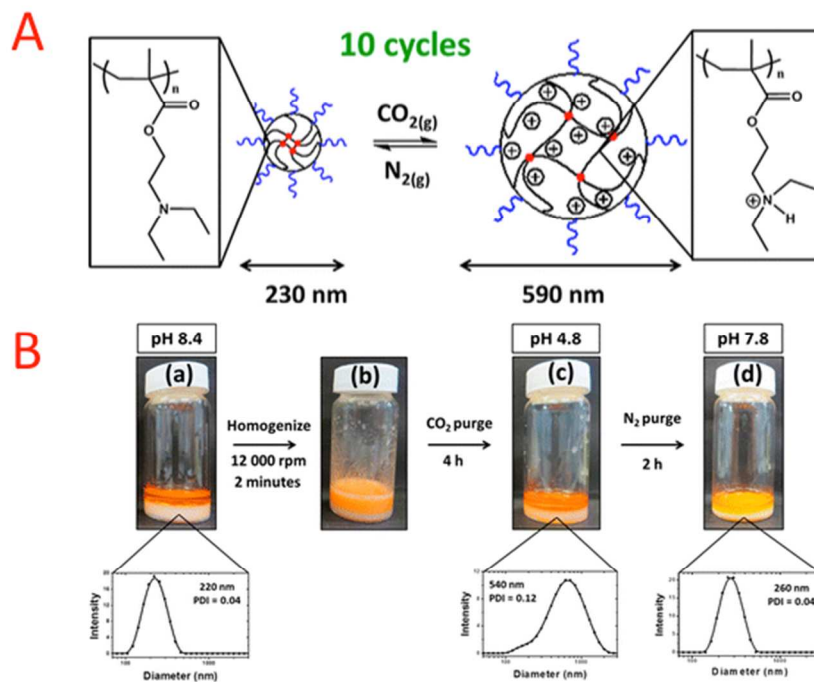


**Figure 10** (A) Schematic illustration representing the  $\text{CO}_2/\text{N}_2$ -responsiveness of PEGMA-PDEAEMA latex particles. (B) (a-d) Digital photographs demonstrating the  $\text{CO}_2/\text{N}_2$  tunable stability of isopropyl myristate-in-water emulsions stabilized PEGMA-PDEAEMA latex particles, with insets indicating the DLS particle size distribution Reprinted with permission from American Chemical Society (ref. 79), Copyright (2005).

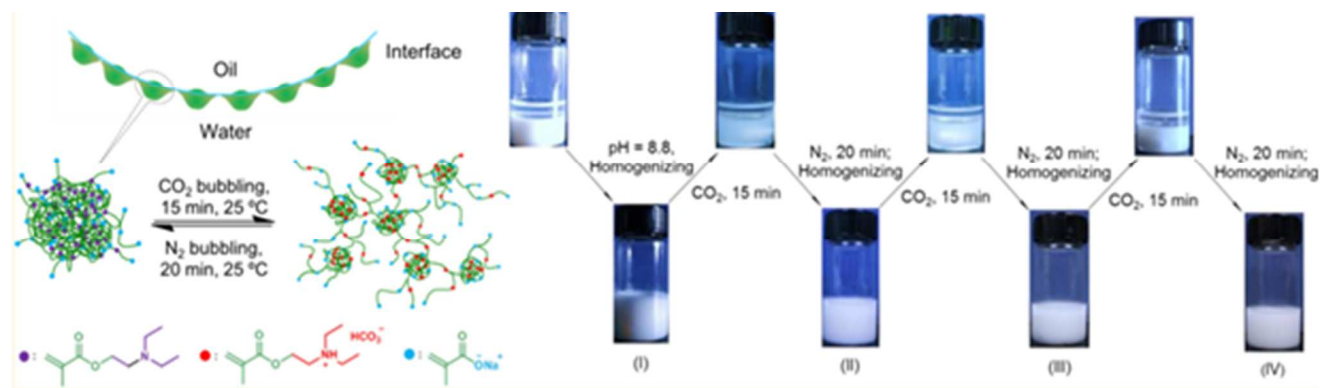


**Figure 11** (Left) Schematic illustration demonstrating the  $\text{CO}_2/\text{N}_2$ -responsive structural modifications observed for crosslinked P(DMAEMA-co-SMA) particles. (Right) Digital photographs demonstrating the  $\text{CO}_2/\text{N}_2$ -responsiveness for *n*-dodecane-in-water emulsions stabilized by crosslinked P(DMAEMA-co-SMA) particles Reprinted with permission from American Chemical Society (ref. 80), Copyright (2014).

**Table 5** Alternative stimuli-responsive Pickering emulsion systems

Stimulus	Particles	Modifiers	References
Magnetic	Carbonyl iron particles		12
Magnetic	Fe <sub>3</sub> O <sub>4</sub> nanoparticles		13
Magnetic	Fe <sub>3</sub> O <sub>4</sub> nanoparticle	Grafting of bromoesterified ethyl cellulose (EC-Br) onto the surface of amino-functionalized magnetite (Fe <sub>3</sub> O <sub>4</sub> ) nanoparticles	83
Magnetic	CNC/CoFe <sub>2</sub> O <sub>4</sub>		84
Ca <sup>2+</sup>	Poly (4-styrenesulfonic acid- <i>co</i> -maleic acid)		85
ClO <sup>4-</sup>	SiO <sub>2</sub> nanoparticles	PMETAC brushes	86
Light	SiO <sub>2</sub> nanoparticles	Piropyran decorated UCNP	87

## 2.4 Alternative responsive Pickering emulsion systems

A number of other stimuli, such as magnetic field, salt concentration, and light intensity have also been investigated for the control of Pickering emulsion stability<sup>12,13,83–87</sup>. Peng and coworkers<sup>83</sup> studied the use of interfacial active polymer coated magnetic nanoparticles to stabilize and separate w/o emulsions. They first coated Fe<sub>3</sub>O<sub>4</sub> nanoparticles with a thin layer of silica, followed by reaction with 3-aminopropyltriethoxysilane (3-APTES) to render the particle surface amine functionalized (Figure 12). They then grafted bromoesterified ethyl cellulose (EC) onto the particles to introduce interfacial activity. Stable w/o emulsions were prepared and droplet coalescence was initiated after the introduction of a magnetic field, resulting in macrophase separation. Removal of the magnetic field allowed the oil phase to be stably redispersed within the water phase. Unmodified Fe<sub>3</sub>O<sub>4</sub> nanoparticle stabilized o/w Pickering emulsions were the subject of work recently reported by Zhou et al.<sup>13</sup>. Dodecane/water and PDMS (low viscosity)/water emulsion systems were prepared and remained stable for up to six months. More polar oils, such as butyl butyrate and decanol, could not be stabilized by the relatively hydrophilic Fe<sub>3</sub>O<sub>4</sub> nanoparticles due to the very low  $\theta_w$  observed for these systems. While not directly investigated by the authors, it is expected that the introduction of an external magnetic field may destabilize the stable emulsion systems. As with thermo sensitive systems, some of the primary advantages of Pickering emulsion systems controlled by magnetic field intensity are their minimal invasiveness, ease of implementation, and scalability.

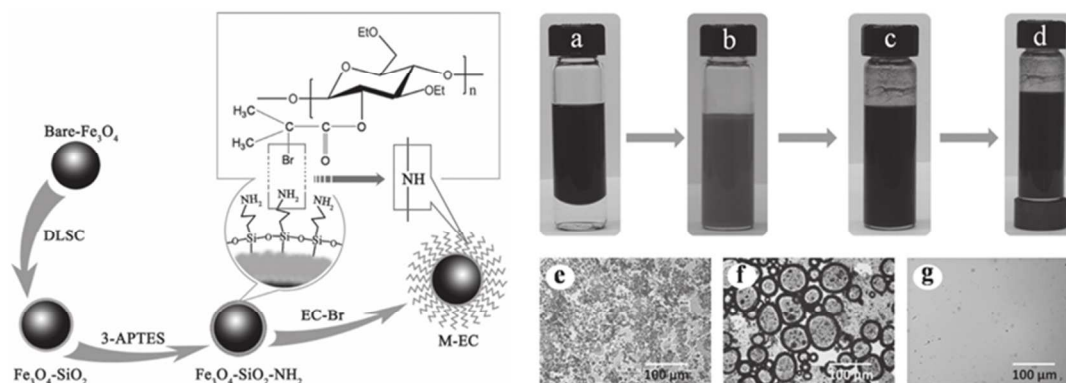


**Figure 12** (Left) Schematic illustration demonstrating the synthetic procedure used to prepare EC grafted magnetic nanoparticles. (Right) (a-d) Digital photographs demonstrating the stabilization and destabilization process of water in asphaltene-in-toluene emulsions using EC grafted magnetic nanoparticles; (e) Microscopy image of solution (b) wherein water is dispersed within an asphaltene-in-toluene emulsion; (f) Microscopy image of solution (c) wherein EC grafted magnetic nanoparticles surround the disperse water droplets and isolate them from the oil phase; (g) Microscopy image of the oil phase of solution (d) wherein the emulsified water droplets have been removed from the oil phase by introduction of a magnetic field Reprinted with permission from John Wiley and Sons (ref. 83), Copyright (2012).

Zhao et al.<sup>85</sup> recently reported on the use of poly(4-styrenesulfonic acid-*co*-maleic acid) (P(SS-*co*-MA)) nanoaggregates as  $\text{Ca}^{2+}$ -responsive Pickering emulsifiers (Figure 13). Since P(SS-*co*-MA) is a hydrophilic polymer, containing strongly ionized SS segments and weakly ionized MA segments, it was observed to completely dissolve within the water phase. However, the addition of  $\text{Ca}^{2+}$  ions above a critical concentration (0.2 M) resulted in the aggregation of the polymer chains to form nanoparticles on the order of 10-40 nm, which proceeded to adsorb at the oil/water interface and stabilize o/w emulsions. Dilution of the system to reduce the amount of  $\text{Ca}^{2+}$  below the critical concentration caused the nanoaggregates to dissociate and detach from the interface, which ultimately led to oil droplet coalescence and macrophase separation. While this method of stimulating emulsion stabilization and destabilization may be suitable for certain circumstances, the continuous dilution of the system does limit its applicability. Continuous cycling would eventually result in appreciable reductions in the oil to water ratio, altering the physical properties of the system.



**Figure 13** (Left) Schematic illustration demonstrating the  $Ca^{2+}$  induced formation of P(SS-*co*-MA) nanoparticles. (Right) Schematic illustration and digital photographs demonstrating the  $Ca^{2+}$  concentration responsiveness of o/w emulsions stabilized by P(SS-*co*-MA) nanoparticles Reprinted with permission from American Chemical Society (ref. 85 ), Copyright (2013)

Light intensity (controlled at different wavelength-near infrared and UV) is another stimulus that has been investigated for the control of Pickering emulsion systems. While not having attracted as much attention as the more conventional stimuli, namely pH, temperature, and  $CO_2$  concentration, it can be fairly advantageous as it is generally non-destructive, precise, and easy to implement. Chen and coworkers<sup>87</sup> demonstrated a conceptually novel system using interfacially active upconversion nanophosphors as colloidal emulsifiers for biocatalytic applications (Figure 14). The surface chemistry of the particles was tuned by conjugating with photochromic sipropyrans, which undergo a hydrophilic-lipophilic conformational change in response to UV and visible light. Upon the introduction of NIR light into the system, the upconversion nanophosphors were observed to become excited and emit UV photons. The emitted UV light triggered the conformational change in the surface grafted photochromic sipropyrans. This caused the surface of the particles to become more hydrophilic, which allowed for the Pickering stabilization of o/w emulsions. Exposure to visible light reversed the conformational change on the surface of the particles and resulted in emulsion phase inversion to w/o. The authors used the Pickering emulsion system to facilitate the enantioselective hydrolysis of mandelonitrile (oil soluble) to (*R*)-(-)-mandelic acid (water soluble) using a model bacterium, *Alcaligenes faecalis* ATCC 8750, which resided in the water phase. They observed a significant improvement in catalytic efficiency, even after cycling. This they attributed in part to reduced substrate inhibition. The phase inversion of the system also improved product, emulsifier, and biocatalyst recovery. Further, the use of light as a stimulus, without any variation in temperature or chemical composition, proved to be gentle, showing little damage toward the biocatalysts. However, the use of light as a stimulus is limited to systems wherein light may pass easily through the entire solution so that it may interact with the entire contents. For turbid systems, wherein light is scattered in all directions by large particles, this may not be possible.

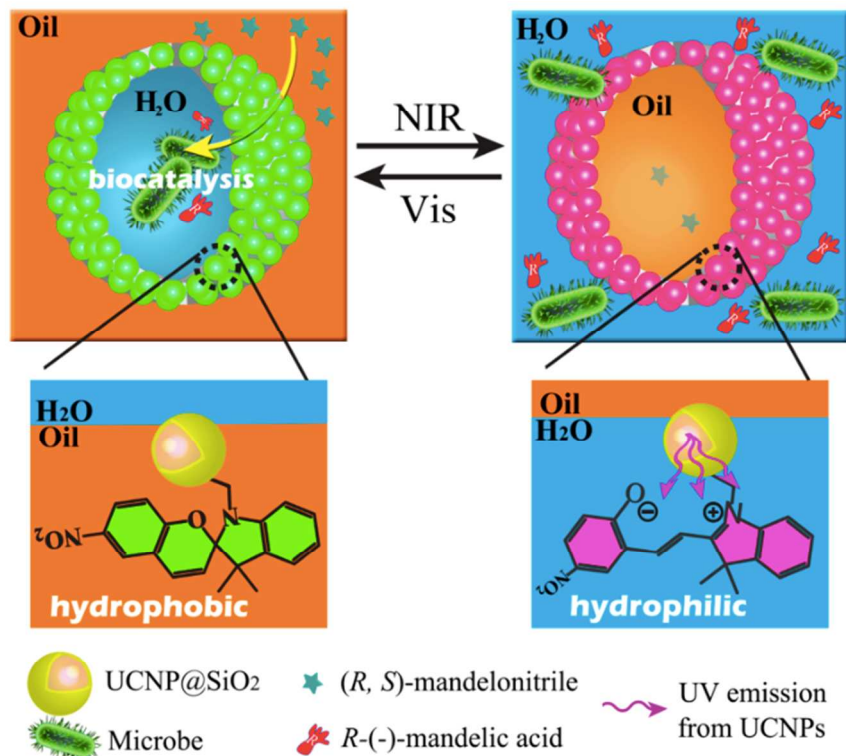


**Figure 14** Schematic illustration demonstrating the NIR/Vis light-responsive phase inversion of emulsions stabilized by photochromic sipropyran conjugated upconversion nanophosphors for more efficient biocatalysis Reprinted with permission from American Chemical Society (ref. 87), Copyright (2014).

**Table 6** Multi-responsive Pickering emulsion systems

Stimuli	Particles	Modifiers	References
Thermo, pH	P(SMA- <i>co</i> -NIPAM) random copolymer		88
Thermo, pH	P(NIPAM-MAA) microgel		89–93
Thermo, pH	Cellulose nanocrystals	PDMAEMA grafted	94
Thermo, magnetic	Fe <sub>3</sub> O <sub>4</sub> -P(NIPAM-MAA) microgel		95
Thermo, ionic strength	Core crosslinked star (CCS) polymers poly(MEA <sub>x</sub> - <i>co</i> -PEGA <sub>y</sub> )*		96
pH, magnetic	Fe <sub>3</sub> O <sub>4</sub> nanoparticle	PAA-PBA coating*	97
Thermo, magnetic	Fe <sub>3</sub> O <sub>4</sub> nanoparticle	PNIPAM	98

\* Poly(MEA<sub>x</sub>-*co*-PEGA<sub>y</sub>): poly(2-methoxyethyl acrylate)-*co*-poly(ethylene glycol) acrylate; PAA-PBA: poly(acrylic acid-*b*-butylacrylate)

## 2.5 Multi-responsive Pickering emulsion systems

Over the past decade, much attention has been devoted to Pickering emulsion systems that respond to more than one stimulus<sup>88–98</sup>. The combination of multiple stimuli is particularly advantageous because it can widen the controllable range or improve the degree of precision of a given system. Presented in Table 6 are a number of multi-responsive Pickering emulsion systems recently reported in the literature.

Given the wide range of stimuli-responsive small molecules and polymers that exist and the unique processing and modification routes available to researchers, a multitude of different multi-responsive systems may be explored. For combined pH and thermo-responsive systems, the most common material investigated has been poly(N-isopropylacrylamide)-*co*-poly(acrylic acid) (P(NIPAM-*co*-MAA)) microgels, which possess both thermo and pH-responsive blocks<sup>89–93</sup>. Early studies by Ngai et al. in 2005<sup>90</sup> showed that P(NIPAM-*co*-MAA) microgel stabilized o/w Pickering emulsions could be destabilized in response to either pH or temperature. Acidification of the system below pH 6 induced the protonation of carboxylate moieties on the PMAA blocks, making the particles more hydrophobic. This caused the microgels to desorb from the interface and diffuse into the oil phase, eventually resulting in droplet coalescence. Similarly, increasing the temperature of the system at pH 6 beyond 60°C induced the coil to globule conformation of PNIPAM segments, making the microgels more hydrophobic and destabilizing the particles at the interface. Interestingly though, the particles remained stable at the interface after an increase in temperature for mildly basic systems, i.e. pH > 8. The authors attributed this observation to the high negative charge density of PMAA blocks in alkaline conditions, which allowed the particles to remain sufficiently hydrophilic and persist at the interface, regardless of molecular conformation. By incorporating Fe<sub>3</sub>O<sub>4</sub> magnetic nanoparticles into the P(NIPAM-*co*-MAA) microgel system, Brugger and Richtering<sup>95</sup> were able to stabilize o/w emulsion of both polar and nonpolar oils. Application of a static magnetic field to the emulsion caused the stable oil droplets to be separated from the continuous water phase without any observed coalescence. The application of a high frequency magnetic field caused an increase in the temperature of the Pickering emulsion, causing the emulsifier to become unstable and detach from the interface, resulting in macrophase separation. In both cases, the dual responsiveness allowed for precise remote control of the Pickering emulsion dynamics. By manipulating the combined effect of temperature and pH of the system, the stabilization/destabilization window could be broadened or narrowed or even shifted as

desired<sup>71,90,95</sup>. Depending on the application, the ability to do so may be advantageous to the operator. Tang and coworkers<sup>94</sup> reported a pH and thermo-responsive system based on PDMAEMA grafted cellulose nanocrystals (CNC) (Figure 15). PDMAEMA possesses a cloud point in the range of 50°C under neutral pH in aqueous solution<sup>81</sup>. However, increasing the pH of the system resulted in a shift of the cloud points to higher temperatures due to the protonation of the amine functionality on the polymer. The authors demonstrated the ability to stabilize both toluene- and heptane-in-water emulsions under basic conditions. The stability of the particles at the interface was attributed to the slightly negative surface charge resulting from the trace sulfate ester moieties present on the surface of CNC. Neutralization of the base caused the protonation of tertiary amine groups of the PDMAEMA chains. The electrostatic interaction between CNC particles and their polymer chains resulted in reversible particle aggregation and emulsion instability. Increasing the temperature of the system beyond 50°C also resulted in demulsification and phase separation. The authors attributed this observation to the stretch-to-collapse transition of the PDMAEMA chains, changing the wettability of the particle surface. In both cases, re-emulsification was possible by adjusting the pH or temperature back to favorable conditions. A thermo and salt-responsive system was recently reported by Chen et al.<sup>96</sup>, wherein a series of core crosslinked poly(2-methoxyethyl acrylate-*co*-poly(ethylene glycol)acrylate) (P(MEA<sub>x</sub>-*co*-PEGA<sub>y</sub>)) were used to stabilize dodecane-in-water high internal phase emulsions (HIPEs). The HIPEs could be thermally triggered to rapidly and completely demulsify at mild temperatures. They also found that addition of kosmotropes, such as Na<sub>2</sub>SO<sub>4</sub>, led to more efficient demulsification, while addition of chaotropes, such as NaSCN, resulted in the opposite effect. Chen and coworkers<sup>98</sup> have recently developed a smart Pickering emulsion system for oil harvesting applications with the ability to respond to temperature and magnetic field intensity (Figure 16). They demonstrated that PNIPAM grafted magnetic composite particles allowed for efficient oil droplet transport within aqueous media. Application of an external magnetic field resulted in separation of the emulsified oil droplets from the water phase and increasing the temperature of the system to 50°C caused the droplets to coalesce.

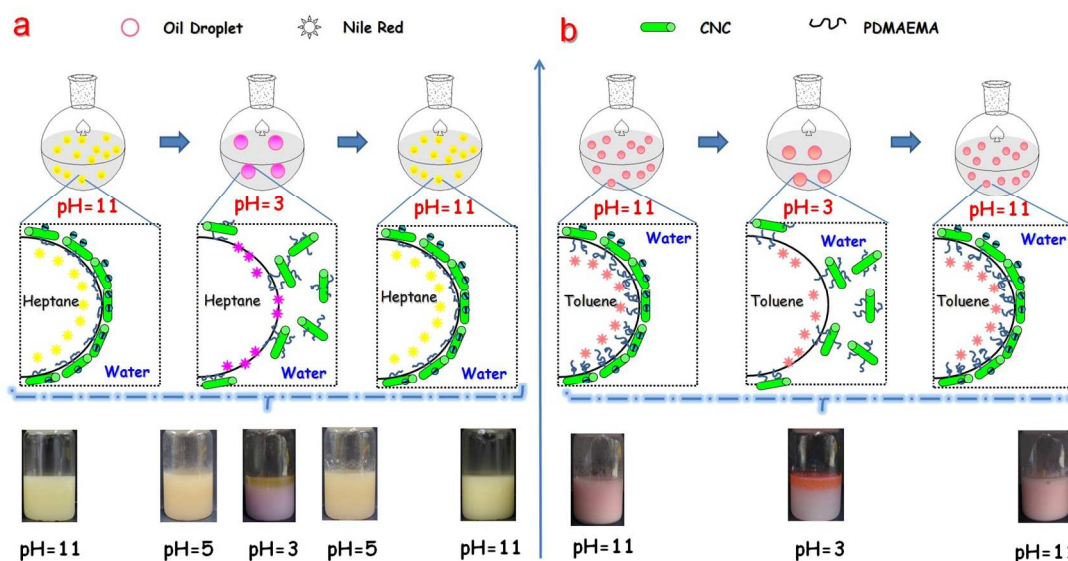


**Figure 15** Schematic illustration and digital photographs demonstrating the pH-responsive behavior of (a) heptane-in-water and (b) toluene-in-water emulsions stabilize by PDMAEMA-g-CNC Reprinted with permission from American Chemical Society (ref. 94), Copyright (2014).

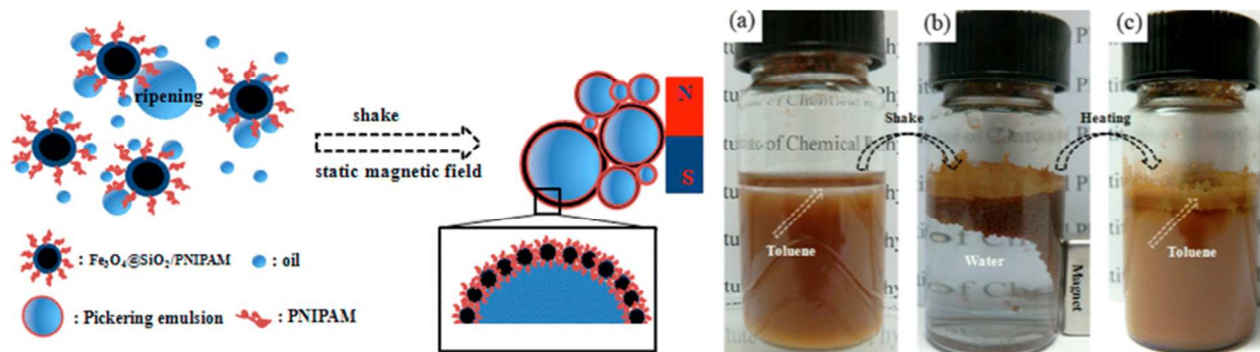


**Figure 16** (Left) Schematic illustration demonstrating the destabilization of an o/w emulsion stabilized by PNIPAM grafted magnetic nanoparticles. (Right) (a-c) Digital photographs demonstrating the two-stage destabilization of a toluene-in-water emulsion responsive to magnetic field intensity and temperature Reprinted with permission from American Chemical Society (ref. 98), Copyright (2014).

### 3 Potential applications

#### 3.1 Pickering emulsion polymerization

Pickering emulsion polymerization was the focus of much scientific research in the 1930s to 1950s,

when polymer chemistry was at the forefront of discovery. While attention to this topic waned over the latter half of the twentieth century, the recent nanotechnology revolution and the desire to develop novel functional nanomaterials has revitalized interest in Pickering stabilized emulsion polymerization<sup>2,23,25,99–104</sup>. Compared to conventional surfactant stabilized emulsion polymerization, Pickering emulsion systems possess a number of advantages, including foam reduction, recyclability, reduced toxicity, and reduced cost<sup>2,20</sup>. By introducing stimuli-responsiveness to Pickering emulsion polymerization systems, emulsions may be instantaneously stabilized and destabilized via an external trigger, allowing for precise control over the degree of polymerization, as well as the simple purification of products and emulsifiers. For instance, pH-responsive alkaline lignin nanoparticles have been used for the emulsion polymerization of styrene<sup>62</sup>. The authors demonstrated the ability to separate and recycle the emulsifier particles multiple times. Specifically, the use of lignin, a waste product from pulp and paper industry, in functional applications such as this is particularly advantageous. Moreover, the high-density solid particle coating imparted by

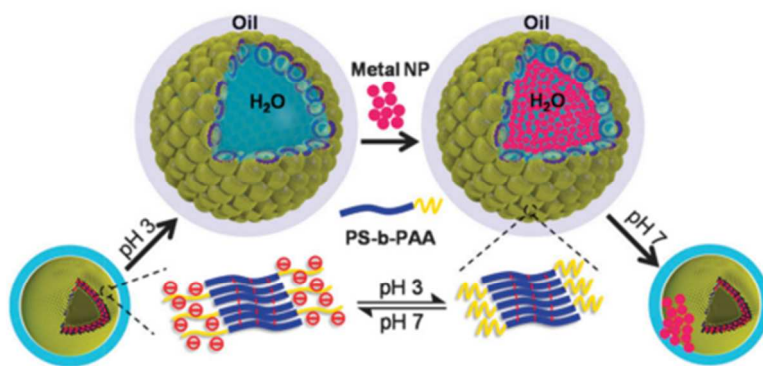


**Figure 17** Schematic illustration demonstrating the fabrication of Janus polymersomes prepared using a pH-responsive polymersome Pickering emulsion Reprinted with permission from Royal Society of Chemistry (ref. 105), Copyright (2014).

Pickering stabilization provides an interesting avenue for fabricating various organic, inorganic, and hybrid functional nanomaterials. For example, Wang and coworkers<sup>105</sup> prepared anisotropic Janus particles by modifying shell crosslinked poly(acrylic acid)-*b*-polystyrene polymersomes with Au and Pt nanoparticles (Figure 17). Under acidic conditions, the pH-responsive polymersomes formed stable w/o emulsion. Introducing metal nanoparticles into the system resulted in the metal nanoparticles migrating to the aqueous phase located on the inside of the emulsion droplets,

wherein they were bound inwardly, on the facing side of the polymersomes. pH adjustment to neutral conditions caused emulsion destabilization. The resulting polymersomes possessed Janus behaviour, with the metal nanoparticles bound to only one side of the surface of the particles. By taking advantage of some of the other stimuli-responsive Pickering emulsifiers described in this review, for example graphene oxide or magnetic nanoparticles, other smart core-shell composite nanomaterials for application as, say, electrorheological or magnetorheological fluids, have also been fabricated<sup>106</sup>.

### 3.2 Enhanced oil recovery

Surfactant-stabilized o/w and w/o emulsions are frequently used in the petroleum industry, in both the flooding and oil recovery processes. The many advantages of stimuli-responsive Pickering emulsions over conventional surfactant-stabilized emulsions, as discussed in previous sections of this review, have widely been applied in food, pharmaceutical, and cosmetic industries. However, their use in the petroleum industry as a substitute for traditional surfactants and amphiphilic polymers has seldom been explored<sup>107–110</sup>. In reservoir flooding processes, it has been suggested that nanoparticle stabilized emulsion droplets are sufficiently small to pass through rock pores without risk of being trapped and may remain stable despite the harsh reservoir conditions due to the irreversible adsorption of the nanoparticles at the emulsion interface<sup>110</sup>. In addition, the high viscosity often observed for Pickering emulsion systems can assist by providing the backpressure necessary to displace and mobilize highly viscous oil, which is difficult for liquid phase transport. Above ground, complex separation operations are used to recover the oil from the process fluids. These separation processes are typically energy intensive and expensive to operate. By incorporating stimuli-responsive Pickering emulsifiers whose stability may be instantaneously controlled via external triggers, it may be possible to both maximize the quantity of oil isolated from mines and enhance the efficiency of the separation and recovery process. In one recent study, hybrid nanoparticles containing a superparamagnetic core and a stimuli-responsive polymer shell have been explored to address the above stated issues<sup>98,111</sup> (Figure 18). The superparamagnetic core provided the particles with stability to resist aggregation during storage, as well as the ability to migrate through the solution in response to an externally applied magnetic field. The pH- and thermo-responsive polymer shell allowed the particles to stabilize and destabilize o/w emulsions on demand. The combination of stimuli-responsive properties of the emulsifier particles provided a simple and effective route for both oil harvesting and particle recovery and recycling..

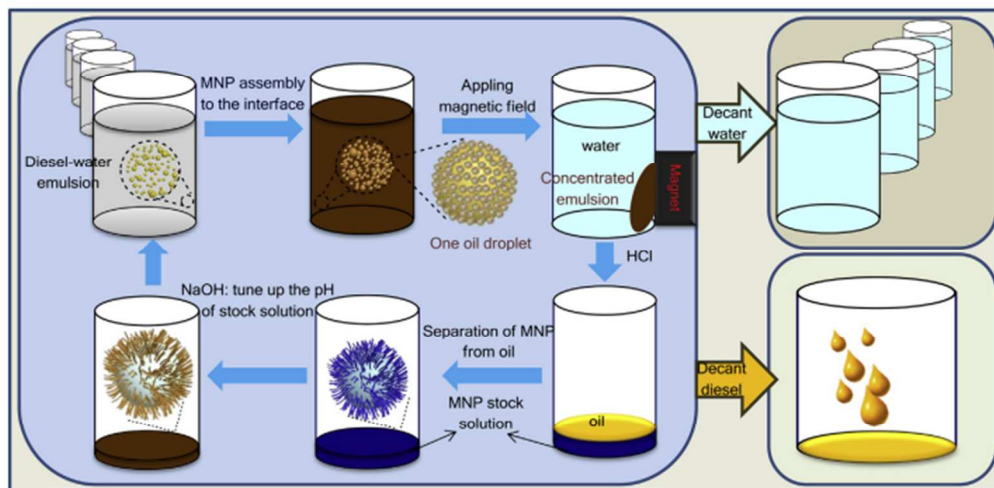


**Figure 18** Schematic illustration demonstrating the application of pH-responsive magnetic nanoparticles as recyclable stabilizers for oil-water separation Reprinted with permission from Elsevier (ref. 111), Copyright (2015)

### 3.3 Catalyst recycling

Biphasic conditions are often required for catalytic reactions and o/w and w/o emulsions are typically used to address this issue<sup>112–115</sup>. In many instances, this is due to the solvent incompatibility of reactants, catalysts, and products. However, the use of emulsions for catalysis has also been observed to provide considerable rate enhancement when compared to single-phase reaction systems. This improvement has been attributed to the compartmentalization and concentration of chemicals participating in the reaction. Although this approach to catalysis has been proven to have potential in many applications, there are a limited number of practical examples reported to date<sup>30,114–116</sup>. The major shortcoming is that conventional emulsion droplets are usually difficult to demulsify after the reaction, which makes it rather challenging to separate the surfactant, catalyst and products after the reaction process. With the help of stimuli-responsive Pickering emulsifiers, it may be possible to harness the improved catalytic efficiency observed for emulsion reaction systems, but also provide enhanced separation of product and catalyst through the direct control of emulsion stability using external stimuli. Two examples of this concept in practice are the work reported by Yang et al.<sup>53</sup> and Chen et al.<sup>87</sup>, which have previously been discussed at length describing pH-responsive and light-responsive Pickering emulsion systems, respectively. Yang et al.<sup>53</sup> investigated the covalent surface functionalization of silica microspheres with

organosilanes for use as heterogeneous solid catalysts that could be repeatedly separated and recycled by phase transfer, while Chen et al.<sup>87</sup> demonstrated a novel system using interfacially active upconversion nanophosphors as colloidal emulsifiers for biocatalytic applications. A recent study by Fang and coworkers<sup>117</sup> has reported on the catalytic reduction of *p*-nitroanisole to *p*-anisidine using o/w microreactors stabilized by Au-functionalized PEO-*b*-P4VP pH-responsive hybrid particles. High catalytic reaction efficiency and simple catalyst separation and recyclability were achieved.

### 3.4 Cosmetic and personal care products

Emulsions are frequently used in the formulations of many cosmetic and personal care products, including skin moisturizers, sunscreen lotion, whitening products, anti-aging products, antiperspirants, deodorants, and hair care products<sup>118,119</sup>. Stimuli-responsive Pickering emulsifiers used in cosmetic and personal care products may increase the stability and shelf life of a given formulation, while permitting the rapid and controlled release of active components when desired in response to triggers like temperature, pH, and light.

## 4 Conclusions and future perspectives

Pickering emulsions possess a number of advantages over traditional surfactant stabilized emulsions, such as enhanced stability, biocompatibility, and environmental friendliness. These characteristics open the door for their use in a variety of industries, spanning petroleum, food, biomedicine, pharmaceuticals, and cosmetics. Depending on the application, rapid, but controlled stabilization and destabilization of an emulsion may be required. This review article provides a comprehensive review of Pickering emulsion systems that possess the ability to respond to an array of external triggers. These include systems that are responsive to pH, temperature, CO<sub>2</sub>, magnetic field intensity, ionic strength, light intensity, and combinations thereof. Many of the works described in this review have demonstrated the ability to rapidly stabilize and destabilize both w/o and o/w emulsions in a well-controlled environment. Some of these systems possess the ability to facilitate complete and reversible phase inversion of o/w to w/o emulsions and vice-versa.

The benefits and disadvantages of various external stimuli have been described throughout in this review. For instance, while pH-responsive systems are well-studied and simple to implement, their repeated use results in the accumulation of salts within the system. Depending on the system and its

sensitivity to ionic strength, this may produce adverse effects. Thermo-responsive systems, on the other hand, are non-accumulative. However, their use for large volumes may not be feasible due to the energy requirements. CO<sub>2</sub>-responsive systems are similar to pH-responsive systems in that they respond to the proton concentration in solution. Like the thermo-responsive systems, though, their use is non-accumulative. One of the primary disadvantages of using CO<sub>2</sub> as a stimulus is the narrow pH window (mildly acidic to neutral) that may be achieved by CO<sub>2</sub> dissolution, and this, ultimately, limits their application. The combination of multiple stimuli is particularly advantageous because it often widens the controllable range or improves the degree of precision of a given system. However, the disadvantages of each system may also be observed when combined.

It is believed that stimuli-responsive Pickering emulsion systems are useful in a number of applications. For instance, their use in emulsion polymerization may permit the instantaneous stabilization and destabilization of the system via an external stimulus. This could provide more precise control over the degree of polymerization. It may also simplify the purification of products and emulsifiers. Ultimately, these improvements have the potential to translate into reduced energy consumption, reduced waste, and improved emulsifier recyclability. By incorporating stimuli-responsive Pickering emulsifiers into oil recovery operations, it may be possible to maximize the quantity of oil isolated from mines by providing a stable and protective sheath for oil droplets in-situ, as well as delivering the back pressure necessary to displace and mobilize highly viscous oil, which would otherwise be unrecoverable. Their use may also enhance the efficiency and recyclability of the above ground oil separation and recovery processes due to their stimuli-responsive behavior. When used in catalysis, stimuli-responsive Pickering emulsifiers make it possible to harness the improved catalytic efficiency observed for emulsion reaction systems, such as increased reaction rate, while also providing enhanced separation of product and catalyst through the direct control of emulsion stability using external stimuli. Lastly, stimuli responsive Pickering emulsifiers used in cosmetic and personal care products may increase the stability and shelf life of a given formulation, while permitting the rapid and controlled release of active components when desired in response to triggers like temperature, pH, and light. The development of functionalized sustainable nanomaterials, such as cellulose nanocrystals offers an attractive opportunity to produce Pickering emulsions using sustainable resources, which are biocompatible, inert and abundant. In addition, such use may contribute to the capture of CO<sub>2</sub> from the environment and offers an attractive strategy to address issues surrounding the global warming of planet earth.

## References:

1. B. Binks, *Curr. Opin. Colloid Interface Sci.*, 2002, **7**, 21–41.
2. A. Schrade, K. Landfester, and U. Ziener, *Chem. Soc. Rev.*, 2013, **42**, 6823–6839.
3. Y. Chevalier and M.-A. Bolzinger, *Colloids Surfaces A Physicochem. Eng. Asp.*, 2013, **439**, 23–34.
4. S. U. Pickering, *J. Chem. Soc.*, 1907, **91**, 2001–2021.
5. W. Ramsden, *Proc. Chem. Soc.*, 1903, **72**, 156–164.
6. D. Dupin, S. P. Armes, C. Connan, P. Reeve, and S. M. Baxter, *Langmuir*, 2007, **23**, 6903–6910.
7. E. Dickinson, *J. Sci. Food Agric.*, 2013, **93**, 710–721.
8. T. N. Hunter, R. J. Pugh, G. V Franks, and G. J. Jameson, *Adv. Colloid Interface Sci.*, 2008, **137**, 57–81.
9. M. Rayner, D. Marku, M. Eriksson, M. Sjöö, P. Dejmek, and M. Wahlgren, *Colloids Surfaces A*, 2014, **458**, 48–62.
10. E. Dickinson, *Curr. Opin. Colloid Interface Sci.*, 2010, **15**, 40–49.
11. M. S. Silverstein, *Prog. Polym. Sci.*, 2014, **39**, 199–234.
12. S. Melle, M. Lask, and G. Fuller, *Langmuir*, 2005, 2158–2162.
13. J. Zhou, X. Qiao, B. P. Binks, K. Sun, M. Bai, Y. Li, and Y. Liu, *Langmuir*, 2011, **27**, 3308–3316.
14. I. Kalashnikova, H. Bizot, B. Cathala, and I. Capron, *Biomacromolecules*, 2012, **13**, 267–275.
15. I. Kalashnikova, H. Bizot, B. Cathala, and I. Capron, *Langmuir*, 2011, **27**, 7471–7479.
16. G. Sun, Z. Li, and T. Ngai, *Angew. Chemie*, 2010, **122**, 2209–2212.
17. H. Katepalli, V. T. John, and A. Bose, *Langmuir*, 2013, **29**, 6790–6797.
18. A. Saha, A. Nikova, P. Venkataraman, V. T. John, and A. Bose, *ACS Appl. Mater. Interfaces*, 2013, **5**, 3094–3100.
19. J. Dong, A. J. Worthen, L. M. Foster, Y. Chen, K. A. Cornell, S. L. Bryant, T. M. Truskett, C. W. Bielawski, and K. P. Johnston, *ACS Appl. Mater. Interfaces*, 2014, **6**, 11502–11513.

20. I. Fuchs and D. Avnir, *Langmuir*, 2013, **29**, 2835–2842.
21. G. Kaptay, *Colloids Surfaces A Physicochem. Eng. Asp.*, 2006, **282-283**, 387–401.
22. H. Duan, D. Wang, N. S. Sobal, M. Giersig, D. G. Kurth, and H. Möhwald, *Nano Lett.*, 2005, **5**, 949–952.
23. T. Chen, P. J. Colver, and S. A. F. Bon, *Adv. Mater.*, 2007, **19**, 2286–2289.
24. D. Li, Y. He, and S. Wang, *J. Phys. Chem. C*, 2009, **113**, 12927–12929.
25. D. J. Voorn, W. Ming, and A. M. van Herk, *Macromolecules*, 2006, **39**, 2137–2143.
26. W. Li, L. Yu, G. Liu, J. Tan, S. Liu, and D. Sun, *Colloids Surfaces A Physicochem. Eng. Asp.*, 2012, **400**, 44–51.
27. F. Yang, Q. Niu, Q. Lan, and D. Sun, *J. Colloid Interface Sci.*, 2007, **306**, 285–295.
28. A. Menner, R. Verdejo, M. Shaffer, and A. Bismarck, *Langmuir*, 2007, **23**, 2398–2403.
29. J. Kim, L. J. Cote, F. Kim, W. Yuan, K. R. Shull, and J. Huang, *J. Am. Chem. Soc.*, 2010, **132**, 8180–8186.
30. X. Huang, M. Li, D. C. Green, D. S. Williams, A. J. Patil, and S. Mann, *Nat. Commun.*, 2013, **4**, 2239.
31. I. Kalashnikova, H. Bizot, P. Bertoncini, B. Cathala, and I. Capron, *Soft Matter*, 2013, **9**, 952–959.
32. M. V. Tzoumaki, T. Moschakis, V. Kiosseoglou, and C. G. Biliaderis, *Food Hydrocoll.*, 2011, **25**, 1521–1529.
33. C. Li, P. Sun, and C. Yang, *Starch - Stärke*, 2012, **64**, 497–502.
34. Z. Nie, J. Il Park, W. Li, S. A. F. Bon, and E. Kumacheva, *J. Am. Chem. Soc.*, 2008, **130**, 16508–16509.
35. A. Dinsmore, M. Hsu, and M. Nikolaidis, *Science*, 2002, **298**, 1006–1010.
36. Y. Chenglin, Y. Yiqun, Z. Ye, L. Na, L. Xiaoya, L. Jing, and J. Ming, *Langmuir*, 2012, **28**, 9211–9222.
37. W. Zhai, G. Li, P. Yu, L. Yang, and L. Mao, *J. Phys. Chem. C*, 2013, **117**, 15183–15191.
38. S. Fujii, S. P. Armes, B. P. Binks, and R. Murakami, *Langmuir*, 2006, **22**, 6818–6825.
39. J. Masliyah, Z. Zhou, and Z. Xu, *Can. J. Chem. Eng.*, 2004, **82**, 628–654.

40. S. Wiese, A. C. Spiess, and W. Richtering, *Angew. Chem. Int. Ed. Engl.*, 2013, **52**, 576–579.
41. Y. Liu, P. Jessop, M. Cunningham, C. Eckert, and C. Liotta, *Science (80-. )*, 2006, **313**, 958–960.
42. S. Dai, P. Ravi, and K. C. Tam, *Soft Matter*, 2008, **4**, 435.
43. J. W. J. de Folter, M. W. M. van Ruijven, and K. P. Velikov, *Soft Matter*, 2012, **8**, 6807.
44. H. Liu, C. Wang, S. Zou, Z. Wei, and Z. Tong, *Langmuir*, 2012, **28**, 11017–11024.
45. S. Fujii, M. Okada, and T. Furuzono, *J. Colloid Interface Sci.*, 2007, **315**, 287–296.
46. D. Yu, Z. Lin, and Y. Li, *Colloids Surfaces A Physicochem. Eng. Asp.*, 2013, **422**, 100–109.
47. J. Li and H. D. H. Stöver, *Langmuir*, 2008, **24**, 13237–12340.
48. J. I. Amalvy, G. F. Unali, Y. Li, S. Granger-Bevan, S. P. Armes, B. P. Binks, J. a Rodrigues, and C. P. Whitby, *Langmuir*, 2004, **20**, 4345–4354.
49. E. S. Read, S. Fujii, J. I. Amalvy, D. P. Randall, and S. P. Armes, *Langmuir*, 2004, **20**, 7422–7429.
50. M. F. Haase, D. Grigoriev, H. Moehwald, B. Tiersch, and D. G. Shchukin, *Langmuir*, 2011, **27**, 74–82.
51. M. F. Haase, D. O. Grigoriev, H. Möhwald, and D. G. Shchukin, *Adv. Mater.*, 2012, **24**, 2429–2435.
52. M. F. Haase, D. Grigoriev, H. Moehwald, B. Tiersch, and D. G. Shchukin, *J. Phys. Chem. C*, 2010, **114**, 17304–17310.
53. H. Yang, T. Zhou, and W. Zhang, *Angew. Chem. Int. Ed. Engl.*, 2013, **52**, 7455–7459.
54. M. Motornov, R. Sheparovych, R. Lupitskyy, E. MacWilliams, O. Hoy, I. Luzinov, and S. Minko, *Adv. Funct. Mater.*, 2007, **17**, 2307–2314.
55. A. J. Morse, J. Madsen, D. J. Growney, S. P. Armes, P. Mills, and R. Swart, *Langmuir*, 2014, **30**, 12509–12519.
56. a J. Morse, D. Dupin, K. L. Thompson, S. P. Armes, K. Ouzineb, P. Mills, and R. Swart, *Langmuir*, 2012, **28**, 11733–11744.
57. S. Fujii, Y. Cai, J. V. M. Weaver, and S. P. Armes, *J. Am. Chem. Soc.*, 2005, **127**, 7304–7305.
58. C. Ma, X. Bi, T. Ngai, and G. Zhang, *J. Mater. Chem. A*, 2013, **1**, 5353–5360.

59. F. Tu and D. Lee, *J. Am. Chem. Soc.*, 2014, **136**, 9999–10006.
60. N. Saleh, T. Sarbu, K. Sirk, G. V Lowry, K. Matyjaszewski, and R. D. Tilton, *Langmuir*, 2005, **21**, 9873–9878.
61. T. Liu, S. Seiffert, J. Thiele, A. R. Abate, D. a Weitz, and W. Richtering, *Proc. Natl. Acad. Sci. U. S. A.*, 2012, **109**, 384–389.
62. Z. Wei, Y. Yang, R. Yang, and C. Wang, *Green Chem.*, 2012, **14**, 3230–3236.
63. A. K. F. Dyab, *Colloids Surfaces A Physicochem. Eng. Asp.*, 2012, **402**, 2–12.
64. J. Tan, J. Wang, L. Wang, J. Xu, and D. Sun, *J. Colloid Interface Sci.*, 2011, **359**, 155–162.
65. X. Liu, C. Yi, Y. Zhu, Y. Yang, J. Jiang, Z. Cui, and M. Jiang, *J. Colloid Interface Sci.*, 2010, **351**, 315–322.
66. Q. Lan, C. Liu, F. Yang, S. Liu, J. Xu, and D. Sun, *J. Colloid Interface Sci.*, 2007, **310**, 260–269.
67. F. Nan, J. Wu, F. Qi, Y. Liu, T. Ngai, and G. Ma, *Colloids Surfaces A Physicochem. Eng. Asp.*, 2014, **456**, 246–252.
68. H. Liu, Z. Zhang, H. Yang, F. Cheng, and Z. Du, *ChemSusChem*, 2014, **7**, 1888–1900.
69. B. P. Binks, R. Murakami, S. P. Armes, and S. Fujii, *Angew. Chem. Int. Ed. Engl.*, 2005, **44**, 4795–4798.
70. C. Monteux, C. Marlière, P. Paris, N. Pantoustier, N. Sanson, and P. Perrin, *Langmuir*, 2010, **26**, 13839–13846.
71. T. Saigal, H. Dong, K. Matyjaszewski, and R. R. D. Tilton, *Langmuir*, 2010, **26**, 15200–15209.
72. S. Tsuji and H. Kawaguchi, *Langmuir*, 2008, **24**, 3300–3305.
73. M. Destribats, V. Lapeyre, M. Wolfs, E. Sellier, F. Leal-Calderon, V. Ravaine, and V. Schmitt, *Soft Matter*, 2011, **7**, 7689.
74. M. Destribats, V. Lapeyre, E. Sellier, F. Leal-Calderon, V. Ravaine, and V. Schmitt, *Langmuir*, 2012, **28**, 3744–3755.
75. J. O. Zoppe, R. a Venditti, and O. J. Rojas, *J. Colloid Interface Sci.*, 2012, **369**, 202–209.
76. J. Jiang, Y. Zhu, Z. Cui, and B. P. Binks, *Angew. Chemie*, 2013, **125**, 12599–12602.
77. C. Liang, Q. Liu, and Z. Xu, *ACS Appl. Mater. Interfaces*, 2014, **6**, 6898–6904.

78. Y. Qian, Q. Zhang, X. Qiu, and S. Zhu, *Green Chem.*, 2014, **16**, 4963–4968.
79. a J. Morse, S. P. Armes, K. L. Thompson, D. Dupin, L. a Fielding, P. Mills, and R. Swart, *Langmuir*, 2013, **29**, 5466–5475.
80. P. Liu, W. Lu, W.-J. Wang, B.-G. Li, and S. Zhu, *Langmuir*, 2014, **30**, 10248–10255.
81. J. Niskanen, C. Wu, M. Ostrowski, G. G. Fuller, S. Hietala, and H. Tenhu, *Macromolecules*, 2013, **46**, 2331–2340.
82. S. Lin and P. Theato, *Macromol. Rapid Commun.*, 2013, **34**, 1118–1133.
83. J. Peng, Q. Liu, Z. Xu, and J. Masliyah, *Adv. Funct. Mater.*, 2012, **22**, 1732–1740.
84. T. Nypelö, C. Rodriguez-Abreu, Y. V Kolen'ko, J. Rivas, O. J. Rojas, N. Carolina, and U. States, *ACS Appl. Mater. Interfaces*, 2014, **6**, 16851–16858.
85. C. Zhao, J. Tan, W. Li, K. Tong, J. Xu, and D. Sun, *Langmuir*, 2013, **29**, 14421–14428.
86. K. Y. Tan, J. E. Gautrot, and W. T. S. Huck, *Langmuir*, 2011, **27**, 1251–1259.
87. Z. Chen, L. Zhou, W. Bing, Z. Zhang, Z. Li, J. Ren, and X. Qu, *J. Am. Chem. Soc.*, 2014, **136**, 7498–7504.
88. C. Yi, N. Liu, J. Zheng, J. Jiang, and X. Liu, *J. Colloid Interface Sci.*, 2012, **380**, 90–98.
89. S. Schmidt, T. Liu, S. Rütten, K.-H. Phan, M. Möller, and W. Richtering, *Langmuir*, 2011, **27**, 9801–9806.
90. T. Ngai, S. H. Behrens, and H. Auweter, *Chem. Commun. (Camb)*, 2005, 331–333.
91. B. Brugger and W. Richtering, *Langmuir*, 2008, **24**, 7769–7777.
92. B. Brugger, B. a Rosen, and W. Richtering, *Langmuir*, 2008, **24**, 12202–12208.
93. W. Richtering, *Langmuir*, 2012, **28**, 17218–17229.
94. J. Tang, M. F. X. Lee, W. Zhang, B. Zhao, R. M. Berry, and K. C. Tam, *Biomacromolecules*, 2014, **15**, 3052–3060.
95. B. Brugger and W. Richtering, *Adv. Mater.*, 2007, **19**, 2973–2978.
96. Q. Chen, Y. Xu, X. Cao, L. Qin, and Z. An, *Polym. Chem.*, 2014, **5**, 175.
97. K. Y. Yoon, Z. Li, B. M. Neilson, W. Lee, C. Huh, S. L. Bryant, C. W. Bielawski, and K. P. Johnston, *Macromolecules*, 2012, **45**, 5157–5166.

98. Y. Chen, Y. Bai, S. Chen, J. Ju, Y. Li, T. Wang, and Q. Wang, *ACS Appl. Mater. Interfaces*, 2014, **6**, 13334–13338.
99. J. Cejková, J. Hanus, and F. Stepánek, *J. Colloid Interface Sci.*, 2010, **346**, 352–360.
100. X. Song, Y. Yang, J. Liu, and H. Zhao, *Langmuir*, 2011, **27**, 1186–1191.
101. H. Hu, H. Wang, and Q. Du, *Soft Matter*, 2012, **8**, 6816.
102. A. Walther, M. Hoffmann, and A. H. E. Müller, *Angew. Chemie*, 2008, **120**, 723–726.
103. D. Yin, L. Ma, J. Liu, and Q. Zhang, *Energy*, 2014, **64**, 575–581.
104. H. Liu, Z. Wei, M. Hu, Y. Deng, Z. Tong, and C. Wang, *RSC Adv.*, 2014, **4**, 29344.
105. Z. Wang, F. P. J. T. Rutjes, and J. C. M. van Hest, *Chem. Commun.*, 2014, **50**, 14550–14553.
106. S. H. Piao, S. H. Kwon, W. L. Zhang, and H. J. Choi, *Soft Matter*, 2015, **11**, 646–654.
107. H. ShamsiJazeyi, C. a. Miller, M. S. Wong, J. M. Tour, and R. Verduzco, *J. Appl. Polym. Sci.*, 2014, **131**, DOI: 10.1002/app.40576.
108. I. Chen, C. Yegin, M. Zhang, and M. Akbulut, *SPE J.*, 2014. SPE 169904
109. A. H. Bornae, M. Manteghian, A. Rashidi, M. Alaei, and M. Ershadi, *J. Ind. Eng. Chem.*, 2014, **20**, 1720–1726.
110. T. Zhang, D. Davidson, S. L. Bryant, and C. Huh, *SPE Improv. Oil Recover. Symp.*, 2013. SPE 129885
111. X. Wang, Y. Shi, R. W. Graff, D. Lee, and H. Gao, *Polymer (Guildf.)*, 2015, 1–7.
112. C. Zhang, C. Hu, Y. Zhao, M. Möller, K. Yan, and X. Zhu, *Langmuir*, 2013, **29**, 15457–15462.
113. G. Scott, S. Roy, Y. M. Abul-Haija, S. Fleming, S. Bai, and R. V Ulijn, *Langmuir*, 2013, **29**, 14321–14327.
114. C. Wu, S. Bai, M. B. Ansorge-Schumacher, and D. Wang, *Adv. Mater.*, 2011, **23**, 5694–5699.
115. Z. Wang, M. C. M. van Oers, F. P. J. T. Rutjes, and J. C. M. van Hest, *Angew. Chem. Int. Ed. Engl.*, 2012, **51**, 10746–10750.
116. S. Crossley, J. Faria, M. Shen, and D. E. Resasco, *Science*, 2010, **327**, 68–72.
117. Z. Fang, D. Yang, Y. Gao, and H. Li, *Colloid Polym. Sci.*, 2015, DOI 10.1007/s00396–015–3533–3538

118. F. G. Hougeir and L. Kircik, *Dermatol. Ther.*, 2012, **25**, 234–237.
119. S. Simonvic, N. Ghouchi-Eskandar, and C. A. Prestidge, *J. Drug. Deliv. Sci. Tec.*, 2011, **21**, 123-133.

TOC:

